Oecologia (1998) 114:441–454

G. James Collatz · Joseph A. Berry · James S. Clark

Effects of climate and atmospheric CO_2 partial pressure on the global distribution of C_4 grasses: present, past, and future

Received: 3 July 1997 / Accepted: 3 December 1997

Abstract C_4 photosynthetic physiologies exhibit fundamentally different responses to temperature and atmospheric CO_2 partial pressures (pCO_2) compared to the evolutionarily more primitive C_3 type. All else being equal, C_4 plants tend to be favored over C_3 plants in warm humid climates and, conversely, C_3 plants tend to be favored over C_4 plants in cool climates. Empirical observations supported by a photosynthesis model predict the existence of a climatological crossover temperature above which C_4 species have a carbon gain advantage and below which C_3 species are favored. Model calculations and analysis of current plant distribution suggest that this pCO_2-dependent crossover temperature is approximated by a mean temperature of 22°C for the warmest month at the current pCO_2 (35 Pa). In addition to favorable temperatures, C_4 plants require sufficient precipitation during the warm growing season. C_4 plants which are predominantly graminoids of short stature can be competitively excluded by trees (nearly all C_3 plants) – regardless of the photosynthetic superiority of the C_4 pathway – in regions otherwise favorable for C_4. To construct global maps of the distribution of C_4 grasses for current, past and future climate scenarios, we make use of climatological data sets which provide estimates of the mean monthly temperature to classify the globe into areas which should favor C_4 photosynthesis during at least 1 month of the year. This area is further screened by excluding areas where precipitation is <25 mm per month during the warm season and by selecting areas classified as grasslands (i.e., excluding areas dominated by woody vegetation) according to a global vegetation map. Using this approach, grasslands of the world are designated as C_3, C_4, and mixed under current climate and pCO_2. Published floristic studies were used to test the accuracy of these predictions in many regions of the world, and agreement with observations was generally good. We then make use of this protocol to examine changes in the global abundance of C_4 grasses in the past and the future using plausible estimates for the climates and pCO_2. When pCO_2 is lowered to pre-industrial levels, C_4 grasses expanded their range into large areas now classified as C_3 grasslands, especially in North America and Eurasia. During the last glacial maximum (~18 ka BP) when the climate was cooler and pCO_2 was about 20 Pa, our analysis predicts substantial expansion of C_4 vegetation – particularly in Asia, despite cooler temperatures. Continued use of fossil fuels is expected to result in double the current pCO_2 by sometime in the next century, with some associated climate warming. Our analysis predicts a substantial reduction in the area of C_4 grasses under these conditions. These reductions from the past and into the future are based on greater stimulation of C_3 photosynthetic efficiency by higher pCO_2 than inhibition by higher temperatures. The predictions are testable through large-scale controlled growth studies and analysis of stable isotopes and other data from regions where large changes are predicted to have occurred.

Key words Photosynthesis · C_4 · Climate change · CO_2 · Grassland

G.J. Collatz (✉)
Code 923, Biospheric Sciences Branch,
NASA's Goddard Space Flight Center,
Greenbelt, MD 20771, USA
e-mail: jcollatz@biome.gsfc.nasa.gov; fax: 301-286-0239

J.A. Berry
Department of Plant Biology,
Carnegie Institution of Washington, Stanford, CA 94305, USA

J.S. Clark
Department of Botany, Duke University,
Durham, NC 27708, USA

Introduction

The core biophysical and biochemical processes of photosynthesis are the same in all higher plants. However, in response to decreases in atmospheric CO_2 partial pressure (pCO_2) over geologic time scales, plants have

evolved different mechanisms by which atmospheric CO_2 is delivered to the primary CO_2-fixing enzyme, ribulose 1,5-bisphosphate carboxylase/oxygenase (Rubisco). C_4 photosynthesis appears to be such an adaptation (Andrews and Lorimer 1987; Ehleringer et al. 1991, in press; Cerling et al. 1993). In C_3 plants which are the more primitive type, CO_2 reaches the site of the Rubisco reaction in the leaf chloroplasts by diffusion across the stomata, the intercellular air spaces, the cell wall and, finally, the membranes of the cell and chloroplasts. The pCO_2 at the site of fixation during active photosynthesis (p_i) is, thus, always lower than the ambient pCO_2. In C_4 plants, CO_2 is delivered to the Rubisco reaction sites by a "CO_2-concentrating mechanism" which maintains pCO_2 many times higher than in the ambient atmosphere during active photosynthesis. This concentrating mechanism requires special complementation of biochemical reactions between cell types and the intercellular transport of metabolites within leaves. Metabolic energy (ATP) derived ultimately from photosynthetic light reactions is required for each CO_2 reaching the site of CO_2 fixation by Rubisco (see Hatch 1987).

Plants with C_3 or C_4 photosynthesis respond differently to ambient conditions of light, temperature, pCO_2, partial pressure of O_2 (pO_2) and humidity (e.g., Björkman and Berry 1973; Collatz et al. 1992). In C_3 plants, the efficiency of solar energy conversion into carbohydrates generally increases with pCO_2 and decreases with temperature. In C_4 plants, on the other hand, photosynthetic efficiency is unaffected by pCO_2 (Ehleringer and Björkman 1977) and may increase with temperature (for high light conditions). The differences between C_3 and C_4 responses to pCO_2 and temperature at the leaf level appear to be expressed at the whole plant and canopy level in CO_2 enrichment experiments (Drake 1991; Polley et al. 1993). If we accept that photosynthetic carbon gain plays a role in determining competitive success, then these differences between C_3 and C_4 physiologies should be reflected in their geographical distributions.

Even before the discovery of the C_4 pathway, global patterns of grass taxa distributions were recognized to correlate with latitude and climate (Hartley 1958, 1973; Hartley and Slater 1960). The structural, physiological, and taxonomic features of C_4 photosynthesis became clear in the 1960s and revealed that tropical grass taxa are largely C_4 while temperate grasses are largely C_3 (Hatch et al. 1968; Downton and Tregunna 1967). The significance of temperature in determining C_4 occurrence has since been corroborated in several studies (e. g., Teeri and Stowe 1976; Rundel 1980; Hattersly 1983). Ehleringer (1978) used an empirical model of photosynthetic temperature responses to account for observed C_3/C_4 grass distributions in the North American Great Plains and Sonoran Desert. He predicted that the carbon gain advantage and, therefore, C_4 dominance in the Great Plains of North America occurred south of 45° N. His regressions of maximum and minimum temperatures to latitude can be used to infer that the mean monthly temperature of the warmest month is 22°C at that latitude. This result compares well with observed distributions in the Great Plains including a floristic study of C_3/C_4 grasses by Teeri and Stowe (1976), biomass measurements compiled by Coupland (1992) and isotopic measurements by Tieszen et al. (1997). Berry and Raison (1981) also suggested a 22°C threshold for C_4 based on altitudinal distributions reported by Rundel (1980).

Though most of the earth's vegetation is C_3 type, model simulations of global CO_2 fluxes suggest that C_4 photosynthesis contributes substantially to the global carbon budget (e.g., Lloyd and Farquhar 1994). Furthermore, C_3 and C_4 photosynthesis also discriminate differently against $^{13}CO_2$ (see Farquhar et al. 1989). Recent analysis of pCO_2 and $^{13}\delta$ CO_2 measurements of the atmosphere have shown that accurate estimates of the contribution of C_4 to global CO_2 fixation over time and space are needed to infer the location and nature of CO_2 sources and sinks (Lloyd and Farquhar 1994; Fung et al. 1997).

Here we present a method for predicting the distribution of C_4 grasses globally based on photosynthetic responses to temperature and CO_2 and apply it using climatological data and estimates of pCO_2 . An extensive literature review of the current distribution of C_4 grasses confirms the accuracy and generality of the approach for the current climate and pCO_2 regime (35 Pa). The approach can be used in modeling studies to either prescribe a global map of photosynthetic type as boundary conditions or to prognosticate distributions during simulations.

In the past, climate and pCO_2 of the earth have varied to the extent that C_4 grass distributions may have been affected. Ehleringer et al. (1991) and Cerling et al. (1993) have argued that C_4 photosynthesis evolved in response to periods of relatively low pCO_2 over 5,000 ka BP. Vostoc ice cores reveal pCO_2 changes of the order of 10 Pa that are positively correlated with temperature variations of about 10°C over the 150 ka BP (Barnola et al. 1987; Jouzel et al. 1987). Since pre-industrial times, pCO_2 has increased by about 8 Pa and will continue to increase in the future, perhaps associated with some climate warming. The impact of these changes on C_4 grass distributions are examined using observed current climate and simulated climates for the last glacial maximum (LGM) and elevated CO_2 "greenhouse" conditions.

Theory

Calculation of and justification for C_3/C_4 crossover temperature

All photosynthetic organisms utilize Rubisco to assimilate CO_2 into the pentose phosphate pathway (PPP) ultimately producing triose phosphates, the primary substrate for synthesis of all organic carbon in the biosphere. Rubisco-catalyzed carboxylation is strongly limited by CO_2 at current ambient partial pressures and

Table 1 Model parameters (see Collatz et al. 1991, 1992) (*PAR* photosynthetically active radiation)

Parameter		Value	Unit
a	PAR absorptance	0.8	–
α_{C_3}	Intrinsic quantum efficiency of C_3 photosynthesis	0.085	mol mol^{-1}
α_{C4}	Intrinsic quantum efficiency of C_4 photosynthesis	0.06	mol mol^{-1}
pO_2	Atmospheric O_2 partial pressure	21,000	Pa
s_{25}	Specificity of Rubisco for CO_2 relative to O_2 at 25°C	2,600	–
Q_{10}	Relative change in s due to 10°C temperature change	0.57	–
pCO_2	Atmospheric CO_2 partial pressure	18–70	Pa
p_i/pCO_2	Ratio of intercellular to atmospheric CO_2 partial pressure	0.8	–

by the presence of O_2, which is an alternate substrate and competitive inhibitor of the carboxylation reaction (see Andrews and Lorimer 1987). At current pCO_2 and pO_2 and 25°C, the maximum rate of net CO_2 fixation by a C_3 plant is only about 20% of the maximum capacity of Rubisco in leaves and about 20% of the photosynthetic light reaction products are used for the unproductive oxygenation reaction (Laing et al. 1974; Collatz et al. 1977; Farquhar et al. 1980). As temperature increases, the affinity of Rubisco for O_2 goes up relative to its affinity for CO_2 causing oxygenation and inhibition of carboxylation to increase with temperature (Badger and Collatz 1977). As a consequence of the oxygenation reaction, all plants exhibit photorespiration in which a product of oxygenation, phosphoglycolate, is metabolized to usable PPP substrates PGA and CO_2. This process diminishes net CO_2 uptake and leads to the consumption of extra ATP and NADPH derived from the light reactions of photosynthesis, thus lowering the effective quantum yield of CO_2 fixation. As noted above, the pCO_2 at the site of the Rubisco reaction is always lower than the ambient atmosphere in C_3 plants because CO_2 is transported by diffusion. The CO_2-concentrating mechanism of C_4 photosynthesis, on the other hand, maintains a high CO_2 partial pressure at the sites of the Rubisco reaction, thus minimizing the impact of photorespiration. High CO_2 results in full utilization of the Rubisco capacity of the leaves in contrast to the 20% utilization typical for C_3 CO_2 fixation. However, the carbon pump in C_4 photosynthesis consumes chemical energy derived from the light reactions of photosynthesis and reduces potential quantum efficiency (see Hatch 1987).

At low irradiances, the efficiency of photon absorption by chlorophyll limits photosynthesis, a process that is relatively insensitive to temperature (Osmond et al. 1980). Studies by Ehleringer and Björkman (1977) showed that the quantum efficiency of CO_2 fixation in C_3 plants is superior to C_4 plants when pCO_2 is elevated or pO_2 is reduced from normal ambient levels. At 30°C and current ambient pCO_2 and pO_2, C_3 and C_4 plants showed similar efficiencies, leading Ehleringer and Björkman to suggest that the cost of the C_4 mechanism was similar to the loss of efficiency in C_3 plants due to photorespiration. They also noted that the C_3 quantum yield for CO_2 fixation decreases as temperature increases while for C_4 it does not change with temperature. Apparently, the stoichiometric energy requirement of the carbon pump in C_4 photosynthesis is insensitive to temperature while increasing temperature alters the kinetics of Rubisco and thus photorespiration and CO_2 fixation in C_3 plants.

These effects were expressed mathematically by Farquhar et al. (1980), who formulated a model of C_3 photosynthesis based on the competitive inhibition kinetics of Rubisco and the stoichiometry of photosynthetic ATP and NADPH generation and consumption. The light-limited rate of photosynthesis (A) is expressed as:

$$A = a\ \alpha_{C_3} I \frac{p_i - \frac{pO_2}{2s}}{P_i + 2\frac{pO_2}{2s}} \quad (1)$$

where a is the absorptance of the leaf to photosynthetically active radiation (PAR), α_{C_3} is the potential maximum (intrinsic) quantum yield of C_3 photosynthesis in the absence of O_2, I is the PAR incident on the leaf surface, p_i is the pCO_2 in the chloroplasts, pO_2 is the partial pressure of O_2 in the chloroplasts, and s is the temperature-dependent specificity of Rubisco for CO_2 relative to O_2 (see Table 1, Appendix). This expression fully explains the temperature and CO_2 dependence of photosynthetic CO_2 fixation by C_3 plants when light is rate limiting.

Figure 1a shows the responses of the effective quantum yield of CO_2 fixation or dA/dI (Eq. 1) to temperature at four pCO_2, 20 Pa representing LGM conditions, 27 Pa for pre-industrial, 35 Pa for current and 70 Pa for double current conditions. These responses include the effects of leaf absorptance (a) and of the pCO_2 gradient between the atmosphere and the sites of carboxylation. For the latter case, the value for p_i was assumed to be equal to $0.8 \times pCO_2$. Instantaneous leaf gas exchange (Wong et al. 1979; Ball and Berry 1982), plant growth measurements (Polley et al. 1993) and analysis of preserved leaf material (Peñuelas and Azcón-Bieto 1992) show that the ratio of p_i to pCO_2 remains relatively constant as pCO_2 varies provided humidity remains constant. The value of 0.8 used here is appropriate for C_3 leaves at high atmospheric humidities (see Wong et al. 1979; Ball and Berry 1982).

The intrinsic quantum yield of C_4 photosynthesis (α_{C_4}) varies among the C_4 plant taxa between 0.052–0.065 mol mol^{-1} but less so for C_4 grass taxa (0.060–0.065 mol mol^{-1} (see Ehleringer et al. in press). This variation may be related to the independent emergence of C_4 photosynthesis in several taxa each with unique

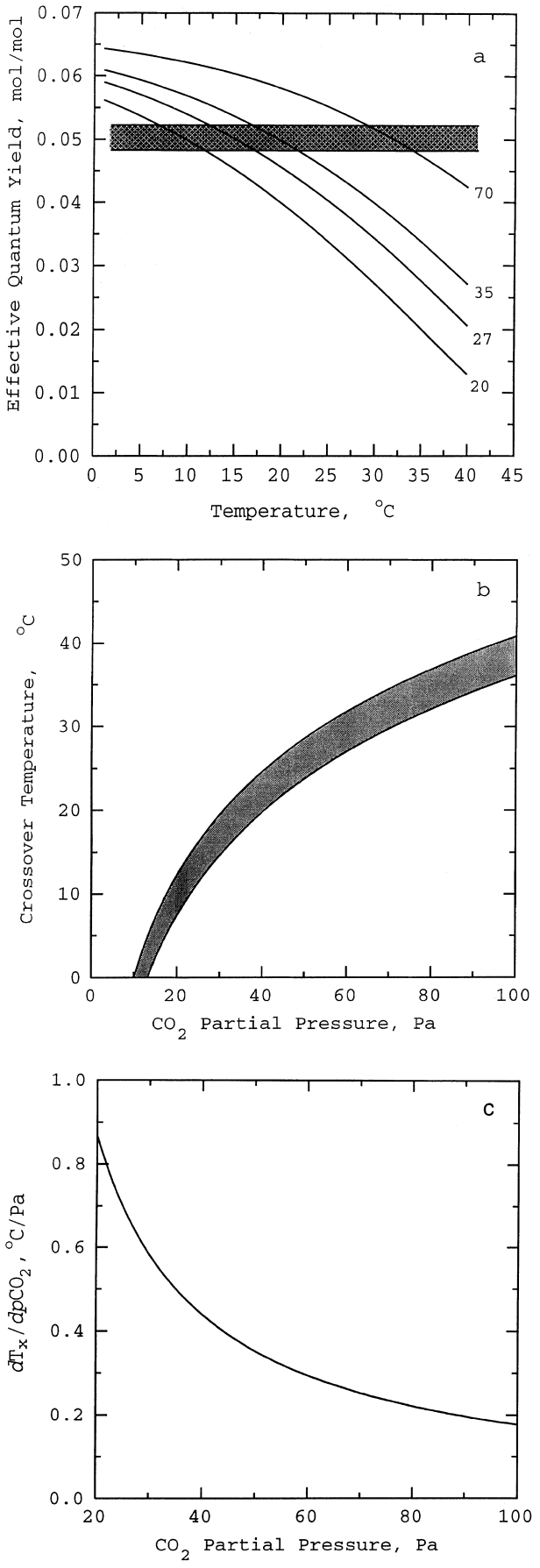

structural and biochemical variations (Ehleringer et al., in press). In all cases, the quantum yield for C_4 photosynthesis does not respond to pCO_2 or non-stressful temperatures. In contrast, there is no indication that α_{C_3} or photorespiration varies much among C_3 plants (Ehleringer et al., in press). The plots shown in Fig. 1a indicate graphically the crossover temperature (T_x) at which C_3 and C_4 species have identical quantum yields for CO_2 fixation. The gray band indicates the mean range observed in α_{C_4} for C_4 grasses causing T_x to vary between 17–22°C at $pCO_2 = 35$ Pa. An analytical expression for T_x is given in the Appendix. Figure 1b shows the strong dependence of T_x on pCO_2 . However, the range in T_x resulting from variation in α_{C_4} (~5°C) is independent of pCO_2. Figure 1c shows the response of the derivative of the crossover temperature formulation with respect to pCO_2 ($dT_x/dpCO_2$) to pCO_2, and the analytical expression is given in the Appendix. Note that this derivative which defines the sensitivity of T_x to pCO_2 depends solely on p_i and the Q_{10} for s. It is not affected by prescribed values of α_{C_3}, α_{C_4}, s, or pO_2.

If we assume that photosynthetic efficiency is important in determining competitive success, then the distributions of these photosynthetic types should respond to variations in climate and pCO_2. The physiological crossover temperature analogy has been used to explain distributions in terms of a climatic crossover temperature, below which C_3 plants will be more efficient and above which C_4 plants will have the photosynthetic advantage (Ehleringer and Björkman 1977; Ehleringer 1978; Berry and Raison 1981). We extend this concept to examine the effects of climate change and associated changes in pCO_2 on the distribution of C_4 plants in the past and future.

Data

Current climate

Current climate (L&C) was prescribed using the Leemans and Cramer (1990) mean monthly temperature and precipitation data set, a compilation from over 13,000 land stations for 1930–1960, and includes an interpolation scheme to correct for altitudinal effects on temperature. The original data at 0.5° × 0.5° spatial resolution was averaged to 1° × 1° to match that of the vegetation maps (see below).

◀

Fig. 1a–c Simulations illustrating the response of the crossover temperature (T_x) for the apparent quantum yield of CO_2 fixation to temperature and different partial pressures of atmospheric CO_2 (pCO_2). Results are corrected for leaf absorptance and diffusion of CO_2. **a** Response of quantum yield of CO_2 fixation to temperature and pCO_2. The C_3 responses are represented by the family of curves at the indicated pCO_2 (Pa). The *gray band* represents the mean range of quantum yields observed for C_4 grasses. **b** T_x as a function of pCO_2. The *gray band* indicates the range of responses associated with the observed range in mean quantum yield of C_4 grasses. **c** The sensitivity ($dT_x/dpCO_2$) as a function of pCO_2

LGM

Simulated temperature and precipitation fields for the LGM ~18 ka BP produced by the GISS GCM (Hansen et al. 1983, 1984) were obtained from the National Oceanographic and Atmospheric Administration (NOAA) Paleoclimatology Program World Wide Web site (http://www.ngdc.noaa.gov/paleo/model.html). According to the accompanying documents, these simulations were run at a horizontal resolution of about $8° \times 10°$ with nine atmospheric layers in the vertical. The boundary conditions for the LGM simulations included ice sheet configuration, sea surface temperatures (SSTs), sea ice 18 ka BP orbital forcing, and $pCO_2 = 20$ Pa. The control simulation used current climatological SSTs, ice, and pCO_2 of 32 Pa.

Doubled atmospheric CO_2

Two simulated mean climates were obtained using SiB2-GCM (Randall et al. 1996; Sellers et al. 1996a, b) with pCO_2 prescribed at 35 and 70 Pa. The model was run at $4° \times 5°$ horizontal resolution, 17-layer vertical resolution at a 6-min time step for 30 simulated years. Vegetation amount, phenology, and type were prescribed at current conditions as estimated from satellite observations (Sellers et al. 1996c). Precipitation and temperatures from the last 10 years of the control and $2 \times CO_2$ runs were averaged to monthly means.

Vegetation map

The global $1° \times 1°$ vegetation data set of Matthews (1983) was used to identify grassland regions of the world. This data set is based on literature surveys and specifies the potential vegetation (excluding human land use change such as agriculture and urbanization). The Matthews grassland biomes were pooled and the resulting map used with C_3/C_4 climate classification to identify C_3, C_4, and mixed grasslands.

Results and discussion

Current C_4 distributions

Figure 2 is a map showing (in red) the regions where we predict C_4 grasses would be equal to or superior to competing C_3 grasses at approximately current pCO_2 (35 Pa) and the current climate as defined by the L&C data set. We constructed this map by selecting those cells where the mean monthly temperature was above 22°C (T_x at $pCO_2 = 35$ Pa, see above) for at least 1 month of the year. These cells are shown in blue or red in Fig. 2. The areas shown in red also met the constraint that at least 25 mm of precipitation occurred in that month. Areas which did not meet this constraint (shown in blue) are regions (deserts and Mediterranean climate regions) where the warm and dry seasons coincide and are unlikely to support C_4 grasses. Note that differences in α_{C_4} among the grasses results in a range of T_x rather than just one value such as 22°C. We have not included this in our analysis since this uncertainty is probably small compared to the uncertainty in the climate data.

The data in Fig. 2 have been combined with vegetation classification maps of Matthews (1983) and DeFries and Townshend (1994) to produce land surface boundary conditions for a general circulation model (Randall et al. 1996; Sellers et al. 1996a, b) and used to study the global atmospheric carbon budget (e.g., Denning et al. 1995; Ciais et al. 1997; Fung et al. 1997). This vegetation map is available to the public on compact disc (Sellers et al. 1996d).

Validation

Our validation approach relied on reported descriptions of plant cover for regions of all the continents. Generally, photosynthetic type is not included in these descriptions but we were able to obtain this information by genus from Watson and Dallwitz (1992). Many of the regional floristic descriptions were obtained from vari-

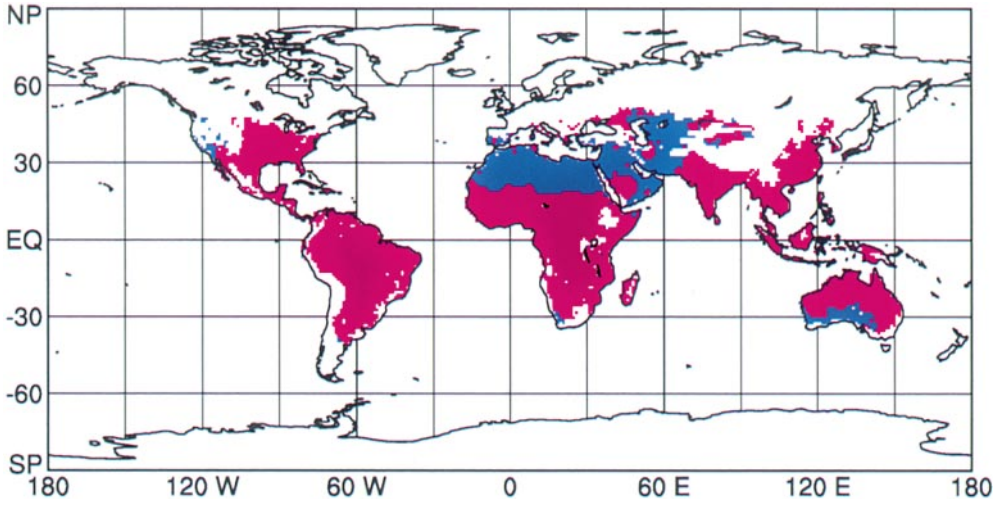

Fig. 2 Map of land surfaces satisfying the "> 22°C for any month" constraint (*red + blue* areas) and satisfying the "> 22°C and > 25 mm precipitation for any month" constraint (*red only* areas). The latter represents the area predicted to have a climate that favors dominance by C_4 grasses over C_3 grasses

Table 2 References used to validate the predicted current distribution of C_4 grasses

Location	Reference
North America	Teeri and Stowe 1976; Coupland 1992; Lauenroth and Milchunas 1992; Tieszen et al. 1997
Africa	Tieszen et al. 1979; Wyk 1979; Werger 1986
Asia	Kawanabe 1979; Walter and Box 1983; Ellis 1992; Lavrenko and Karamysheva 1993; Ting-Cheng 1993
Australia	Hattersley 1983
Europe	Knapp 1979
Hawaii	Rundel 1980
Japan	Kawanabe 1979; Takeda et al. 1985a; Takeda 1988
South America	Soriano 1983, 1992
Global	Hartley 1958, 1973; Hartley and Slater 1960; Nix 1983

ous volumes in the *Ecosystems of the world* series (e.g., Nix 1983; Coupland 1992; Soriano 1983, 1992). A literature survey (Table 2) of the global distributions of grass genera according to photosynthetic type revealed that the most consistent criterion for the occurrence of C_4 grass genera was mean temperature $>22°C$ and mean precipitation >25 mm for any month. Non-grass herbaceous taxa such as the Cyperaceae show a similar climate-dependent distribution of C_3 and C_4 species (Takeda et al. 1985b).

Discrepancies between predictions and reported occurrence were mostly caused by errors in the climate data. For example, the Tamarin Basin in central Asia is misclassified as favoring C_4 grasses because L&C precipitation estimates are too large for this region (as compared to data from Walter and Box 1983).

Low-temperature intolerance has been proposed to explain the predominance of the C_4 type in warm climates (see Long 1983), although C_4 photosynthesis is not entirely excluded from cool and cold climates. C_4 shrubs, for instance, are a significant component of the Great Basin region of the central-western USA (Caldwell et al. 1977a, b). C_4 plants are also a major component of high-latitude coastal salt marshes and C_4 grasses occur in the boreal forest zone of North America (Schwarz and Redmann 1988). In all of these environments, soil salinity may confer some as yet unknown advantage to C_4 over C_3, allowing C_4 species to extend into regions in which they are at a quantum yield disadvantage.

It has been noted that growing season minimum temperatures are sometimes better than maximum temperatures for predicting C_4 distributions (see Long 1983). This may in part be because minimum growing season temperatures are often positively correlated with atmospheric humidity and precipitation (Teeri and Stowe 1976). In other words, warm dry climates will tend to have lower growing-season minimum temperatures than warm wet climates. The minimum precipitation constraint used here will tend to reject areas with low growing-season minimum temperatures.

Classification of grasslands

The regions delineated in Fig. 2 as C_4 are not necessarily dominated by C_4 vegetation. Where resources permit, competition for light leads to dominance by tall vegetation. With some exceptions, C_4 plants are of short stature and concentrated among the grass taxa. This means that, if resources such as water and nutrients permit trees to grow, then the C_3 trees will outcompete C_4 grasses for light, as is the case for tropical forests. An exception that seems to support the rule is the bamboo subfamily, which is one of the few C_3 grass taxa that is well represented in topical and subtropical climates (Takeda 1988) and is also the only grass taxon with species that grow to tree height and are capable of outcompeting short C_4 grasses for light. When tropical forests are removed by logging in Amazonia, C_4 grasses become dominant components of the early regrowth (Nobre et al. 1991).

Global maps of vegetation classifications can be used to identify where grasslands occur within the climate domains predicted by the temperature and precipitation constraints. One such map (Matthews 1983) assigns about 25% of the ice-free land surface as grassland biomes and of that about 57% is C_4 based on our criteria and the L&C climate. C_4 is generally absent from grasslands in the north, at higher elevations, and in Mediterranean climate regions. African grasslands are largely C_4, Asian largely C_3, and in North and South America, both C_3 and C_4 grasslands are well represented.

Some grasslands classified here as C_4 have months of the year that are cooler than 22°C but warm and wet enough to support C_3 species. Seasonal changes in the relative C_4 dominance have been described, especially in the Great Plains region of North America (e.g., Sellers et al. 1992, Tieszen et al. 1997; see also Syverson et al. 1976; Werger 1986). We can predict where C_3/C_4 should vary seasonally by identifying grasslands in which some monthly temperatures are at or below the crossover temperature of 22°C and precipitation is greater than 25 mm. In Fig. 3a, "C_4 only" (shown in red) are grassland grid cells where all months have mean temperatures $>22°C$ and more than 25 mm precipitation. "C_3 only" (shown in blue) are those grasslands with mean temperatures and precipitation never greater than 22°C and 25 mm, respectively, for the same month. About 1% of all grassland grid points, mostly located in the Andean and Himalayan regions, had no monthly temperature

►

Fig. 3 Distribution of C_3 and C_4 grass based on L&C climatology and the land classification scheme of Matthews (1983). The *upper panel* shows the areas corresponding to C_3 (*blue*), C_4 (*red*), and mixed C_3C_4 (*yellow*) grasslands based on the $T_x = 22°C$, corresponding to $pCO_2 = 35$ Pa (~current levels). The *lower panel* shows the corresponding distributions based on $T_x = 18°C$, corresponding to $pCO_2 = 27$ Pa (~pre-industrial CO_2 levels). The *middle panel* is the difference between the pre-industrial and present distributions. Areas shown in *green* are predicted to have changed from mixed C_3C_4 to C_4 and areas shown in *red* to have changed from C_4 to C_3

A. 35 Pa

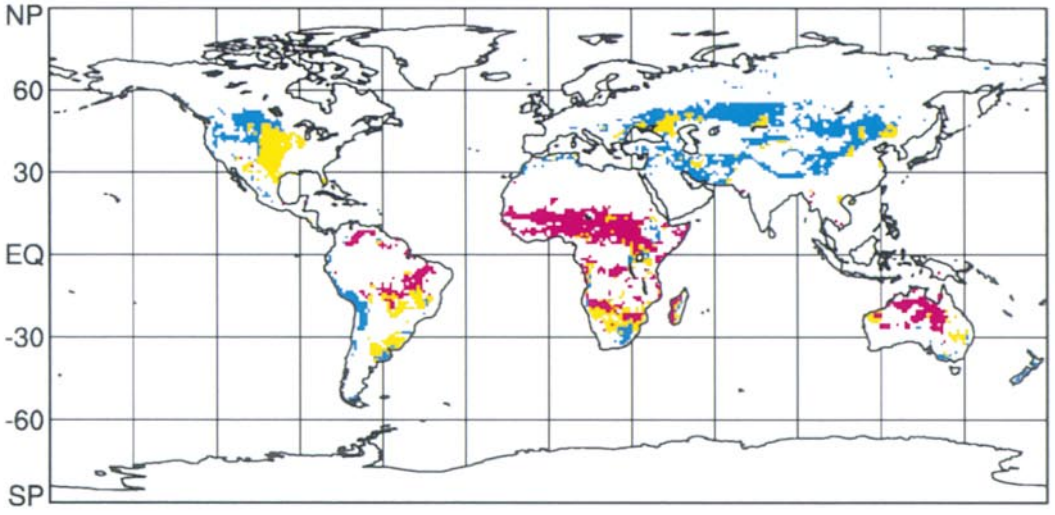

B. Difference (C - A)

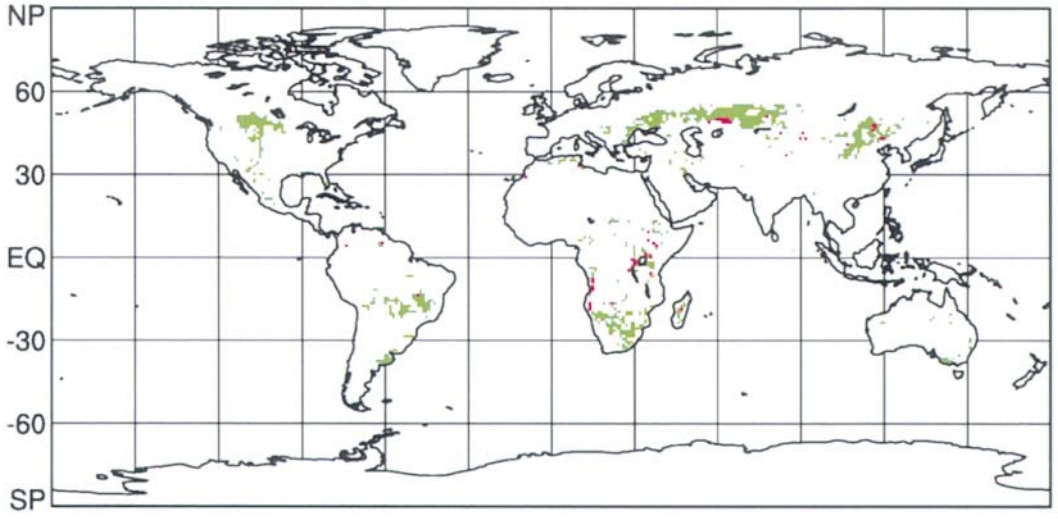

C. 27 Pa

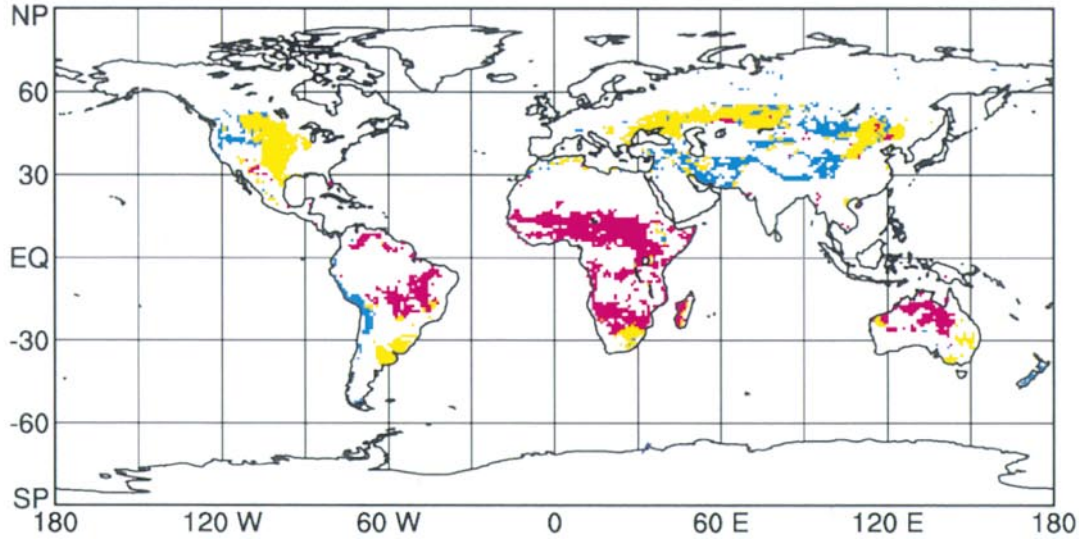

above 0°C with >25 mm of precipitation. Mixed C_3C_4 grasslands (shown in green) have months that satisfy the precipitation constraint above and below 22°C. Mixed grasslands are most evident in the western hemisphere and their occurrence is consistent with floristic descriptions in the literature (North America: Teeri and Stowe 1976; Tieszen et al. 1997; South America: Soriano1992). The South African and eastern and western Asian grasslands are also predicted to support seasonally varying mixtures of C_3 and C_4 grasses.

Influence of atmospheric CO_2 on C_4 distributions for current climate and vegetation

There is remarkable though possibly fortuitous agreement between the observed C_4 distributions and the crossover temperature for current pCO_2 predicted by our model (Appendix 1, Fig. 1a, b). According to the model, climate warming would favor expansion of C_4 grasses whereas increasing pCO_2 would favor C_3 grasses. Substantial pCO_2 and climatic temperature changes have occurred in the past and will continue in the future. By combining climate data (observed and simulated) with the physiological crossover temperature model we infer ecological fitness and, thus, past and future distributions of grass photosynthetic types.

One implication of this analysis is that recent increases in pCO_2 (~8 Pa since pre-industrial times) should have substantially altered the global distribution of C_4 grasses. At pre-industrial CO_2 levels (~27 Pa, the model predicts a T_x of 18°C and produces the map shown in Fig. 3C assuming no change in climate or vegetation type. The occurrence of C_4 grasses is predicted to have decreased from 74% to 57% of the total grassland area as a result of the increase in pCO_2 (Fig. 3B). In particular, large regions of the North American Central Plains and Central Asian steppe are predicted to have changed from mixed C_3C_4 to C_3 grasslands following the rise in pCO_2. This result did not change appreciably if we included the estimated 1°C warming over the last century.

How much of the surface of the earth is favorable for C_4 grass dominance depends on the response of T_x to pCO_2 and on the availability of land area meeting the temperature and precipitation requirements. Figure 4 shows a frequency distribution of land area classified according to the mean temperature of the warmest month with >25 mm of precipitation. The solid line shows all land area, and the area under this curve is normalized to 1.0. The dashed line shows the corresponding areas classified as grasslands, which comprise about 25% of the total land area. The vertical lines in Fig. 4 are the values of T_x at pCO_2 = 20, 27, 35, and 70 Pa. The fraction of area that would be classified as C_4 under different CO_2 levels is represented by the area under the curves and to the right of the respective lines. At very low and very high pCO_2 (low and high crossover temperatures, respectively), C_4 fractional area changes are small because few places on the globe show such extreme maximum temperatures. Greatest sensitivity occurs when the T_x changes around the middle of the frequency distribution (15–30°C, Fig. 4).

Figure 5 shows the cumulative land area that exceeds the T_x calculated from pCO_2 as well as land area and grassland area that also satisfy the precipitation constraint (>25 mm). The result is the fraction of land area or grassland area that is predicted to favor C_4 grasses as a function of pCO_2. The C_4 fractional grassland area

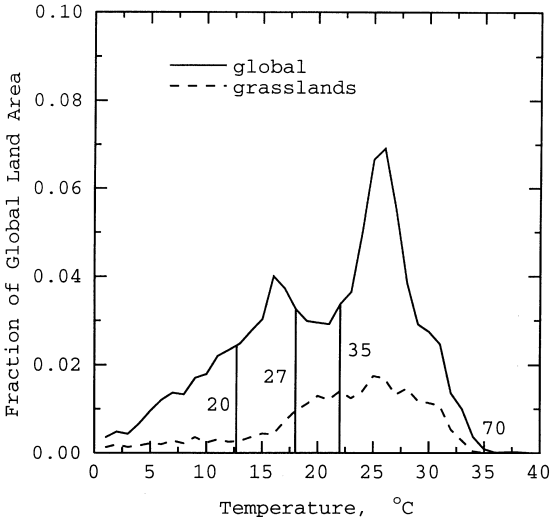

Fig. 4 The frequency distribution expressed as fraction of global land area versus the warmest growing-season month (precipitation >25 mm). The frequency of global grassland area in relation to warmest growing-season temperature is also shown. The *vertical lines* represent the crossover temperature (T_x) for the indicated atmospheric-pCO_2 (Pa). The area under the curves and to the right of the crossover temperature line represents the total land and grassland areas predicted to be favorable to C_4 dominance

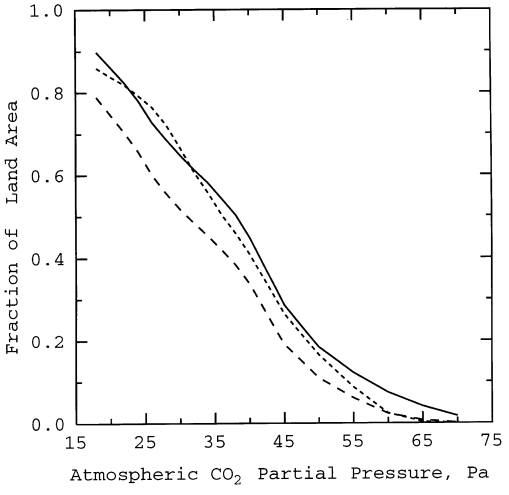

Fig. 5 The frequency of climates favoring C_4 grasses (expressed as fraction of global land area) as a function of atmospheric pCO_2. The fraction of global land area with temperatures warm enough and fractions of global land area (*long-dash line*) and grassland area (*short-dash line*) that are warm and wet enough to favor C_4 grasses are also shown

and global land area decreased in parallel from about 0.8 to 0 as pCO_2 is increased from LGM levels to $2 \times$ current pCO_2. The precipitation constraint removes a relatively constant fraction of the global land area from C_4 climate designation ($\sim$0.1). Grasslands follow the global trends with greatest sensitivity occurring at around the current value of pCO_2.

At a $pCO_2 = 20$ Pa (and current climate), more than 70% of world grasslands would be C_4, while at $2 \times$ present CO_2 (and current climate), very little if any grasslands would be C_4. However, these estimates do not take into account changes in climate. For example, when the pCO_2 was 20 Pa during the last glacial maximum, land temperatures were substantially cooler, and when pCO_2 reaches 70 Pa in the next century, land temperatures are expected to be warmer. These changes in temperature would tend to counter the impact of pCO_2. We have analyzed simulated climates to address this issue.

LGM climate

Mean precipitation and temperatures for January and July produced by the GISS GCM using LGM and current boundary conditions were used to estimate the net change in the distribution of C_4 climate. The control simulation produces a map (not shown) that is in general similar to that produced from the L&C climatology (Fig. 2). Mean of January and July land surface temperatures for the control simulation (0 ka BP) were similar to L&C mean for the year (12.4°C vs 12.7°C, respectively) as were the C_4 fractions of total land area (0.43 and 0.44, respectively).

The land surface was $\sim$7°C cooler (annual mean) in the simulated LGM climate. Taken by itself this would be expected to lead to a reduction in the area available for C_4 species, but the lower pCO_2 (20 Pa) that prevailed during the LGM would be expected to lead to expansion of the C_4 area. Our model suggests that the net effect of these opposing forces was a slight contraction of the area favoring C_4 from the LGM (0.53) to the present (0.43). Figure 6 is a map showing the difference in C_4 distribution between the LGM and the control simulations. Areas where C_4 species may have advanced during the LGM are shown in red. In general, our analysis predicts an expansion of C_4 species at high latitudes during the LGM. This is evident on all of the continents except North America where the cooling due to the ice sheet was apparently sufficient to offset the effect of lowered pCO_2. This result is consistent with arguments recently put forward by Ehleringer et al. (in press), and they suggest that it may be possible to test these predictions by analysis of the carbon isotopes in paleosols and sediment cores that span this transition.

A twofold pCO_2 climate

The dominant role of pCO_2 changes in determining C_4 grass distributions implied in the above analysis has significant implications for future distribution, given projected increases in pCO_2. As shown in Fig. 5, the land area held by C_4 plants should decrease sharply with increasing pCO_2, assuming that climate does not also change. To examine the possible impact of climate change on this result, we have examined a pair of GCM runs with control (35 Pa) and $2 \times pCO_2$ (70 Pa) forcing (Sellers et al. 1996a). The radiative forcing resulted in a 1.9°C increase in the mean land surface temperature of the $2 \times pCO_2$ treatment (R) relative to the control (C). The frequency distribution of the mean monthly temperature of the warmest month with >25 mm precipitation is plotted for the two treatments in Fig. 7. The control simulation (C) yields a slightly warmer mean temperature for the land surface (24.3°C) than the L&C climatology (21.0°C), but there is no significant change in the shape of the profile. Radiative forcing shifts the frequency distribution, but there is no disproportionate increase in the land area with warm temperatures.

Climate versus CO_2

Figure 8 shows the cumulative area that would be dominated by C_4 species (according to our model) as a function of pCO_2 for all of the climate scenarios examined in this study. As discussed above, there is a strong tendency for C_4 to expand with decreasing pCO_2. This is partially counteracted by the cooler temperatures that co-occurred with low pCO_2 at the LGM. On the other hand, climatic warming predicted to occur with $2 \times pCO_2$ is not expected to compensate for the increase in pCO_2. In all scenarios, C_4 plants should be largely replaced by competing C_3 species. It is well known that there has been extensive invasion of grasslands by shrubs (e.g., Polley et al. 1994). While there is no consensus as to the cause(s) for this invasion, it is significant that this is generally a replacement of C_4 grasses with C_3 shrubs. Cole and Monger (1994), for example, used carbon and oxygen isotope measurements to infer that a C_4-grass-dominated region in the south-western USA shifted to C_3 shrubs in the Holocene largely as a result of increased atmospheric pCO_2 rather than climate changes during that period. It is clear that pCO_2 will continue to increase well into the next century but other climatic feedbacks such as parallel increases in aerosols or cloudiness appear to be moderating the "greenhouse" warming (e.g., Santer et al. 1996), further favoring C_3 expansion globally into the future.

Caveats

The model we propose here is based on the assumption that changes in the value of T_x will lead to changes in the land area occupied by C_3 and C_4 grasses. While the exact value of T_x depends on the quantum yield of the C_4 species considered, it is significant to note that the sensitivity of T_x ($dT_x/dpCO_2$; Fig. 1c) is independent of the

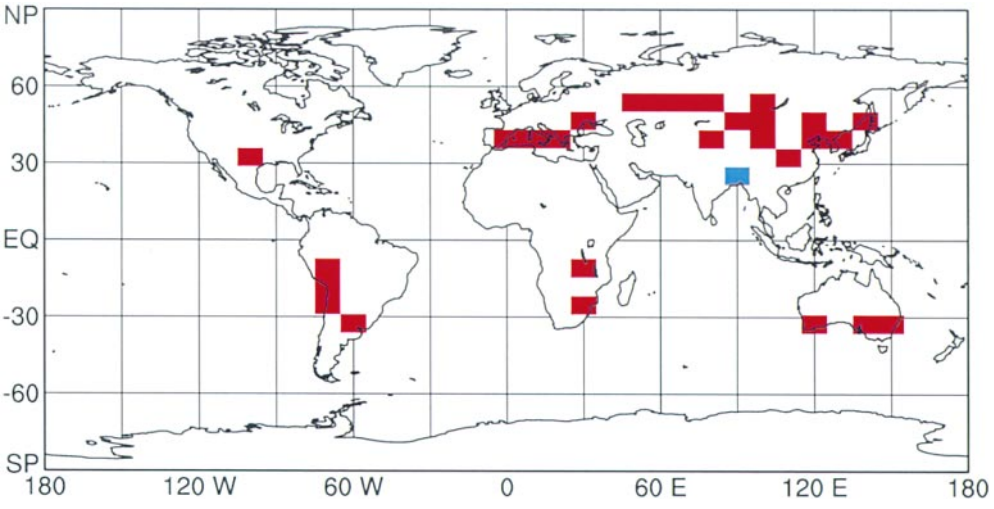

Fig. 6 Map showing areas that changed from C_4 to C_3 (*red*) and from C_3 to C_4 (*blue*) since the last glacial maximum (20 ka BP) as a result of the combined increases in temperature and atmospheric pCO_2. Climate conditions were derived from climate model simulations

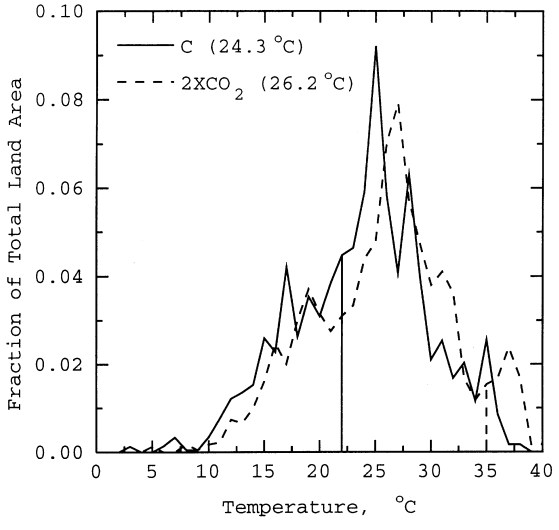

Fig. 7 The frequency of global land area (expressed as fractional land area) versus temperature of the warmest growing-season month for the control (*solid line*) and $2 \times CO_2$ (*dashed line*) simulated climates. The mean temperatures for the warmest growing-season month are shown in parentheses. The *vertical lines* indicate the crossover temperature associated with each scenario. The area under the curve and to the right of the crossover temperature line represents the total area predicted to favor C_4 grasses

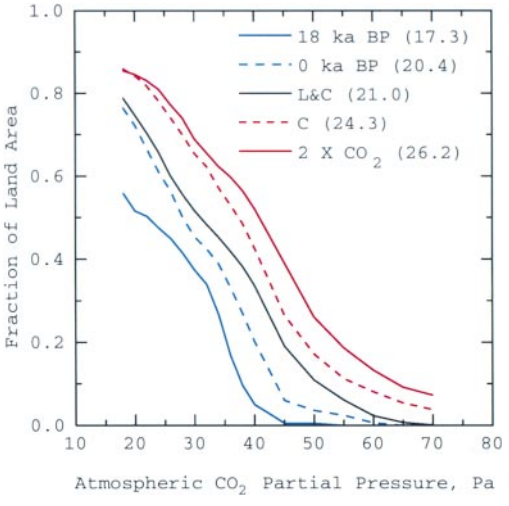

Fig. 8 Response of global land area classified as C_4 climate to atmospheric pCO_2 for various simulated climates and the observed mean climate (*black solid line*). The last glacial maximum (*blue*) and $2 \times CO_2$ (red) climates are the *solid lines*, while their respective control climates (0 ka BP and C) are shown as *dashed lines*. The means for the warmest growing-season month for each climate are shown in parentheses

C_4 quantum yield. The sensitivity of T_x to pCO_2 is determined by p_i and the temperature dependence of the parameter, s. The latter is a property of the enzyme, Rubisco, and there is evidence that this is a conservative kinetic property (Jordan and Ogren 1983; Berry et al. 1994). If the theory that CO_2 fixation efficiency determines competitive success is correct, this should be a robust relationship. We acknowledge, however, that there are obvious weaknesses in this simple theoretical approach. These include:

(1) The relationship described in Eq. 1 applies to light-limited photosynthesis. Under some conditions, photosynthesis may be limited by other processes such as the activity of Rubisco with different temperature and CO_2 sensitivities (Farquhar et al. 1980). In both C_3 and C_4 plants, there is a gradual transition from limitation due to light absorption to Rubisco limitation ($dA/dI \rightarrow 0$) as irradiance increases (Collatz et al. 1990, 1991, 1992). In general, however, PAR limits or co-limits CO_2 fixation over most of the naturally occurring range of PAR (Woodrow and Berry 1988; Collatz et al. 1990). Optimality theory and some empirical observations indicate that most carbon gain occurs under conditions in which photosynthesis is partially limited by both PAR and Rubisco (Field 1988; Farquhar 1989; Sellers et al. 1992a). Even when PAR is not limiting photosynthesis, the differences in responses to pCO_2 and temperature are qualitatively preserved; C_4 photosynthesis tends to be more efficient at higher temperatures and lower pCO_2.

(2) The calculated crossover temperature is sensitive to the estimation of an effective global p_i for C_3 plants. Ehleringer and Cerling (1995) discuss evidence for the consistency of p_i/pCO_2 in response to past changes in pCO_2. In the real world, p_i will vary as the humidity of the atmosphere varies, low humidities resulting in lower stomatal conductance and p_i (Lloyd and Farquhar 1994) causing the crossover temperature to decrease. Low-humidity-induced stomatal closure also occurs in C_4 plants but because of lower sensitivity to CO_2 we expected no significant effect on T_x. The relatively high value for p_i/pCO_2 (0.8) used here (Table 1) lies between ratios close to 1 when A is low at low light and ratios of 0.5 that may occur during light-saturated A at low atmospheric humidities. Lower p_i/pCO_2 would imply greater increases in water use efficiency but the significance for the competitive interaction of C_3 and C_4 plants is not clear because the same factors should also increase the water use efficiency of C_4 plants (Polley et al. 1994).

(3) The climatic mean monthly temperature underestimates the typical daytime temperature at which photosynthesis operates.

(4) The distributions are assumed to always be in equilibrium with changing climate and pCO_2 resulting in no lags. Because of more frequent disturbance and shorter species life spans typical of grassland, it is likely that grasslands will respond faster than woody vegetation types to these environmental changes.

(5) Other ecological factors such as soil salinity may be more important than quantum yield advantage in determining the relative fitness of C_3 and C_4 species. C_3 grasses grow successfully in warm tropical regions with excess water such as marshes (*Phragmites*) and agriculture systems (rice). C_4 grasses do occur in cool climates but are generally restricted to saline soils. Competition for light, soil nutrition, grazing, fires, and so on, could also influence relative fitness.

(6) Non-grass C_4 taxa can be an important component of woody shrub vegetation in some areas (e.g., Caldwell et al. 1977a, b). In general, our analysis should apply to the distribution of herbaceous C_4 taxa (e.g., *Amaranthus*, *Carex*). Woody C_4 plants are generally restricted to saline soils and we have neither a model that considers salinity in determining relative fitness nor the necessary global data sets.

Conclusions

Here, we present a strategy for predicting the distribution of C_4 grasses using monthly mean temperature and precipitation. The crossover temperature approach is simple, it has a biological (mechanistic) interpretation, and it makes predictions that are inherently testable. The predicted current distribution of photosynthetic types in grasslands of the world can be verified through field observations. Previous distributions (i.e., pre-industrial, LGM) may be inferred from the analysis of the isotopic composition of relic organic matter. For instance, analysis of $\delta^{13}C$ composition in environments where terrestrial organic matter has been preserved, e.g., mires (Sukumar et al. 1993) and paleosols (Cerling et al. 1989; Quade et al. 1989; Ambrose and Sikes 1991; Cole and Monger 1994) can identify the relative prevalence of C_4 photosynthesis. Ehleringer et al. (in press) cite examples of measured decreases in $\delta^{13}C$ of preserved organic matter as climate and atmospheric conditions changed since the LGM. These shifts in $\delta^{13}C$ values in the paleo record, however, could be caused by changes either between C_3 and C_4 in grasslands or by changes in vegetation type such as between C_4 grasslands and C_3 woodlands. Shifts in $\delta^{13}C$ values cannot be taken as an unambiguous indicator of shifts in T_x since changes in the precipitation regime might, for example, result in the replacement of C_4 grasses with C_3 trees without a change in T_x. A combination of pollen, ^{18}O, ^{13}C, and ^{14}C measurements could perhaps provide information on vegetation type, temperatures, C_4 dominance, and age, respectively. If we are correct in assuming that photosynthetic carbon gain plays a role in determining the competitive success of grasses, and that our model captures the mechanisms which control carbon gain in C_3 and C_4 species, then it follows that there have been, and will continue to be, large-scale changes in the abundance of C_4 plants in the world. This could be one of the more easily measured responses of the biosphere to global climate change.

Acknowledgements Support for this work was provided by NASA Earth Observing System (EOS) Interdisciplinary Science Program.

APPENDIX We defined the crossover temperature (T_x) as the temperature at which the quantum yield for photosynthetic CO_2 fixation is equal for C_3 and C_4 photosynthesis. The T_x can be expressed mathematically as the temperature at which the derivative of photosynthesis with respect to incident PAR flux (dA/dI) is equal for both C_3 and C_4 photosynthesis. A formulation for light-limited CO_2 fixation in C_4 plants is given by Collatz et al. (1992):

$$A = a\ \alpha_{C_4} I \tag{A1}$$

where A is the photosynthetic CO_2 fixation rate, a is the leaf absorptance for PAR, α_{C_4} is the intrinsic quantum yield for C_4 photosynthesis and I is the PAR incident on the leaf surface. By setting dA/dI of Eq. 1 and A1 equal and defining the specificity (s) in Eq. 1 as:

$$s = 2,600\ Q_{10}^{\frac{T_x - 25}{10}} \tag{A2}$$

s_{25} is the value of s at 25°C and Q_{10} is the relative change in s for a 10°C change in temperature T_x is then defined as:

$$T_x = \frac{10}{\ln Q_{10}} \ln\left(\frac{pO_2}{p_i\ s_{25}} \frac{1 + 0.5\frac{\alpha_{C_3}}{\alpha_{C_4}}}{\frac{\alpha_{C_3}}{\alpha_{C_4}} - 1}\right) \tag{A3}$$

where α_{C_3} is the intrinsic quantum yield for C_3 photosynthesis and p_i is the leaf internal pCO_2 assumed to be equal to 0.8 × atmospheric pCO_2.

Using parameters from Table 1, Eq. A3 produces response of T_x to pCO_2 shown in Fig. 1b. The derivative of Eq. A3 with respect to pCO_2 is:

$$\frac{dT_x}{dp_i} = \frac{10}{\ln Q_{10}} \frac{-1}{p_i} \quad \text{(A4)}$$

and its response to pCO_2 is shown in Fig. 3c.

References

Ambrose SH, Sikes NE (1991) Soil carbon isotope evidence for Holocene habitat change in the Kenya Rift Valley. Science 253: 1402–1405

Andrews TJ, Lorimer GH (1987) Rubisco structure, mechanisms and prospects for improvements. In: Hatch MD, Broadman NK (eds) The biochemistry of plants. Academic Press, Orlando, Fl, pp 131–218

Badger MR, Collatz GJ (1977) Studies on the kinetic mechanism of ribulose-1,5-bisphosphate carboxylase and oxygenase reactions, with particular reference to the effect of temperature on the kinetic parameters. Carnegie Inst Washington Year 76: 355–361

Ball JT, Berry JA (1982) The C_i/C_a ratio: a basis for predicting stomatal control of photosynthesis. Carnegie Inst Washington Year 81: 88–92

Barnola JM, Raynaud D, Korotkevich YS, Lorius C (1987) Vostok ice core provides 160,000-year record of atmospheric CO_2. Nature 329: 408–414

Berry JA, Raison JK (1981) Responses of macrophytes to temperature. In: Lange OL, Nobel PS, Osmond CB, Ziegler H (eds) Encyclopedia of plant physiology. New series, vol. 12A. Springer, Berlin Heidelberg New York, pp 277–338

Berry JA, Collatz GJ, Guy RD, Fogel MD (1994) The compensation point: can a physiological concept be applied to global cycles of carbon and oxygen. In: Tolbert NE, Preiss J (eds) Regulation of atmospheric CO_2 and O_2 by photosynthetic carbon metabolism. Oxford University Press, Oxford, pp 234–248

Björkman O, Berry J (1973) High-efficiency photosynthesis. Sci Am 229: 80–93

Caldwell MM, Osmond CB, Nott DL (1977a) C_4 pathway photosynthesis at low temperature in cold-tolerant *Atriplex* species. Plant Physiol 60: 157–164

Caldwell MM, White RS, Moore TR, Camp LB (1977b) Carbon balance, productivity, and water use of cold winter desert shrub communities dominated by C_3 and C_4 species. Oecologia 29: 275–300

Cerling TE, Quade J, Wang Y, Bowman JR (1989) Carbon isotopes in soils and palaeosols as ecology and palaeoecology indicators. Nature 341: 138–139

Cerling TE, Wang Y, Quade J (1993) Expansion of C_4 ecosystems as an indicator of global ecological change in the late Miocene. Nature 361: 344–345

Ciais P, Denning AS, Tans PP, Berry JA, Randall DA, Collatz GJ, Sellers PJ, White JWC, Trolier M, Meijer HJ, Francey RJ, Monfray P, Heimann M (1997) A three dimensional synthesis study of ^{18}O in atmospheric CO_2. Part 1: surface fluxes. J Geophys Res 102: 5857–5872

Cole DR, Monger HC (1994) Influence of atmospheric CO_2 on the decline of C_4 plants during the last deglaciation. Nature 368: 533–536

Collatz GJ (1977) Influence of certain environmental factors on photosynthesis and photorespiration in *Simmondsia chinensis*. Planta 134: 127–132

Collatz GJ, Berry JA, Farquhar GD, Pierce J (1990) The relationship between the Rubisco reaction mechanism and models of photosynthesis. Plant Cell Environ 13: 219–225

Collatz GJ, Ball JT, Grivet C, Berry JA (1991) Physiological and environmental regulation of stomatal conductance, photosynthesis and transpiration: a model that includes a laminar boundary layer. Agric For Meteorol 54: 107–136

Collatz GJ, Ribas-Carbo M, Berry JA (1992) Coupled photosynthesis-stomatal conductance model for leaves of C_4 plants. Aust J Plant Physiol 19: 519–538

Coupland RT (1992) Mixed prairie. In: Coupland RT (ed) Ecosystems of the world, Vol 8A. Natural grasslands: introduction and western hemisphere. Elsevier, Amsterdam, pp 151–182

DeFries RS, Townshend JRG (1994) NDVI-derived land cover classification at global scales. Int J Remote Sensing 15: 3567–3586

Denning AS, Fung IY, Randall D (1995) Latitudinal gradient of atmospheric CO_2 due to seasonal exchange with land biota. Nature 376: 240–243

Downton WJS, Tregunna EB (1968) Carbon dioxide compensation – its relation to photosynthetic carboxylation reaction, systematics of the Gramineae, and leaf anatomy. Can J Bot 46: 207–215

Drake BG (1991) Canopy photosynthesis of crops and native plant communities exposed to long-term elevated carbon dioxide. Plant Cell Environ 14: 853–860

Ehleringer JR (1978) Implications of quantum yield differences on the distribution of C_3 and C_4 grasses. Oecologia 31: 255–267

Ehleringer J, Björkman O (1977) Quantum yields for CO_2 uptake in C_3 and C_4 plants. Plant Physiol 59: 86–90

Ehleringer JR, Sage RF, Flanagan LB, Pearcy RW (1991) Climate change and the evolution of C_4 photosynthesis. Trees 6: 95–99

Ehleringer JR, Cerling TE (1995) Atmospheric CO_2 and the ratio of intercellular to ambient CO_2 concentrations in plants. Tree Physiol 15: 105–111

Ehleringer JR, Cerling TE, Helliker BR (in press) C_4 photosynthesis, atmospheric CO_2, and climate. Oecologia

Ellis J (ed) (1992) Grasslands and grassland sciences in northern China. National Academy Press, Washington

Farquhar GD (1989) Models of integrated photosynthesis of cells and leaves. Phil Trans R Soc Lond B Biol Sci 323: 357–367

Farquhar GD, Caemmerer S von, Berry JA (1980) A biochemical model of photosynthetic CO_2 assimilation in leaves of C_3 species. Planta 149: 78–90

Farquhar GD, O'Leary MH, Berry JA (1982) On the relationship between carbon isotope discrimination and intercellular carbon dioxide concentration in leaves. Aust J Plant Physiol 9: 121–137

Farquhar GD, Ehleringer JR, Hubick KT (1989) Carbon isotope descrimination and photosynthesis. Annu Rev Plant Physiol. Plant Mol Biol 40: 503–537

Field C (1988) On the role of photosynthetic responses in constraining the habitat distribution of rainforest plants. Aust J Plant Physiol 15: 343–347

Fung I, Field CB, Berry JA, Thompson MV, Randerson JT, Malmström CM, Vitousek PM, Collatz GJ, Sellers PJ, Randall DA, Denning AS, Badeck F, John J (1997) Carbon-13 exchanges between the atmosphere and the biosphere. Global Biogeochem Cycles 11: 507–533

Hansen J, Russell G, Rind D, Stone P, Lacis A, Lebedeff S, Reudy R, Travis L (1983) Efficient three-dimensional global models for climate studies. Mon Weather Rev 111: 609–662

Hansen J, Lacis A, Rind D, Russell G, Stone P, Fung I, Ruedy R, Lerner J, (1984) Climate Sensitivity: analysis of feedback mechanisms. In: Climate processes and climate sensitivity, geophysical monograph 29, Maurice Ewing vol. 5. American Geophysical Union, Washington DC

Hartley W (1958) Studies on the origin, evolution and distribution of the Gramineae. I. The tribe Andropogoneae. Aust J Bot 6: 115–128

Hartley W (1973) Studies on the origin, evolution and distribution of the Gramineae. V. The subfamily Festucoideae. Aust J Bot 21: 201–234

Hartley W, Slater C (1960) Studies on the origin, evolution and distribution of the Gramineae. III. The tribes of the subfamily Eragrostoideae. Aust J Bot 8: 256–273

Hatch MD (1987) C_4 photosynthesis: a unique blend of modified biochemistry, anatomy and ultra structure. Biochim Biophys Acta 895: 81–106

Hatch MD, Slack CR, Johnson HS (1967) Further studies on a new pathway of photosynthetic carbon dioxide fixation in sugarcane and its occurrence in other plant species. Biochem J 102: 417–422

Hattersley PW (1983) The distribution of C_3 and C_4 grasses in Australia in relation to climate. Oecologia 57: 113–128

Jordan DB, Ogren WL (1983) Species variation in kinetic properties of ribulose 1,5-bisphosphate carboxylase/oxygenase. Arch Biochem Biophys 227: 425–433

Jouzel J, Lorius C, Petit JR, Genthon C, Barkov NI, Kotlyakov VM, Petrov VM (1987) Vostoc ice core: a continuous isotopic temperature record over the last climatic cycle (160,000 years). Nature 329: 403–408

Kawanabe S (1979) The pattern of temperature response and its ecological significance. In Numata M (ed) Ecology of grasslands and bamboolands in the world. Junk, The Hague, pp 153–162

Knapp R (1979) Distribution of grasses and grasslands in Europe. In: Numata M (ed) Ecology of grasslands and bamboolands in the world. Junk, The Hague, pp 111–123

Laing WA, Ogren WL, Hageman RH (1974) Regulation of soybean net photosynthetic CO_2 fixation by interaction of CO_2, O_2 and ribulose 1,5-bisphosphate carboxylase. Plant Physiol 54: 678–685

Lauenroth WK, Milchunas DG (1992) Short-grass steppe. In: Coupland RT (ed) Ecosystems of the world, vol 8A. Natural grasslands: introduction and western hemisphere. Elsevier, Amsterdam, pp 183–226

Lavrenko EM, Karamysheva ZV (1993) Steppes of the former Soviet Union and Mongolia. In: Coupland RT (ed) Ecosystems of the world, vol 8B. Natural grasslands: eastern hemisphere and resume. Elsevier, Amsterdam, pp 3–59

Leemans R, Cramer WP (1990) The IIASA database for mean monthly values of temperature, precipitation and cloudiness of a global terrestrial grid. WP-41, International Institute for Applied Systems Analyses, Laxenburg

Lloyd J, Farquhar GD (1994) $\delta^{13}C$ discrimination during CO_2 assimilation by the terrestrial biosphere. Oecologia 99: 201–215

Long SP (1983) C_4 photosynthesis at low temperatures. Plant Cell Environ 6: 345–363

Matthews E (1983) Global vegetation and land use: new high-resolution data bases for climate studies. J Climate Appl Meteorol 22: 474–487

Nix HA (1983) Climate of tropical savannas. In: Bourliere F (ed) Ecosystems of the world, Vol 13. Tropical savannas. Elsevier, Amsterdam, pp 37–62

Nobre CA, Sellers PJ, Shukla J (1991) Amazonian deforestation and regional climate change. J Climate 4: 957–988

Osmond CB, Björkman O, Anderson DJ (1980) Physiological processes in plant ecology: toward a synthesis with *Atriplex*. Springer, Berlin Heidleberg NewYork

Peñuelas J, Azcón-Bieto J (1992) Changes in leaf $\Delta^{13}C$ of herbarium plant species during the past 3 centuries of CO_2 increase. Plant Cell Environ 15: 485–489

Polley HW, Johnson HB, Marino BD, Mayeux HS (1993) Increase in C_3 plant water-use efficiency and biomass over glacial to present carbon dioxide concentrations. Nature 361: 61–64

Polley HW, Johnson HB, Mayeux HS (1994) Increasing CO_2: comparative responses of the C-4 grass *Schizachyrium* and grassland invader *Prosopis*. Ecology 75: 976–988

Quade J, Cerling TE, Bowman JR (1989) Development of Asian monsoon revealed by marked ecological shift during the latest Miocene in northern Pakistan. Nature 342: 163–166

Randall DA, Dazlich DA, Zhang C, Denning AS, Sellers PJ, Tucker CJ, Bounoua L, Berry JA, Collatz GJ, Field CB, Los SO, Justice CO, Fung I (1996) A revised land-surface parameterization (SiB2) for atmospheric GCMs. Part III. The greening of the Colorado State University general circulation model. J Climate 9: 738–763

Rundel PW (1980) The ecological distribution of C_4 and C_3 grasses in the Hawaiian Islands. Oecologia 45: 354–359

Santer BD, Taylor KE, Wigley TML, Johns TC, Jones PD, Karoly DJ, Mitchell JFB, Oort AH, Penner JE, Ramaswamy V, Schwarzkopf MD, Stouffer RJ, Tett S (1996) A search for human influences on the thermal structure of the atmosphere. Nature 382: 39–46

Schwarz AG, Redmann RE (1988) C_4 grasses from the boreal forest region of northwestern Canada. Can J Bot 66: 2424–2430

Sellers PJ, Berry JA, Collatz GJ, Field CB, Hall FG (1992a) Canopy reflectance, photosynthesis and transpiration. III. A reanalysis using improved leaf models and a new canopy integration scheme. Remote Sensing Environ 42: 1–20

Sellers PJ, Heiser MD, Hall FG (1992b) Relations between surface conductance and spectral vegetation indices at intermediate (100 m^2 to 15 km^2) length scales. J Geophy Res 97: 19,033–19,059

Sellers PJ, Bounoua L, Collatz GJ, Randall DA, Dazlich DA, Los SO, Berry JA, Fung I, Tucker CJ, Field CB, Jensen TG (1996a) Comparison of radiative and physiological effects of double atmospheric CO_2 on climate. Science 271: 1402–1406

Sellers PJ, Randall DA, Collatz GJ, Berry JA, Field CB, Dazlich DA, Zhang C, Colello GD, Bounoua L (1996b) A revised land-surface parameterization (SiB2) for atmospheric GCMs. Part I. Model formulation. J Climate 9: 676–705

Sellers PJ, Los SO, Tucker CJ, Justice CO, Dazlich DA, Collatz GJ, Randall DA (1996c) A revised land-surface parameterization (SiB2) for atmospheric GCMs. Part II. The generation of global fields of terrestrial biophysical parameters from satellite data. J Climate 9: 706–737

Sellers PJ, Meeson BW, Closs J, Collatz J, Corprew F, Dazlich D, Hall FG, Kerr Y, Koster R, Los S, Mitchell K, McManus J, Myers D, Sun K-J, Try P (1996d) The ISLSCP Initiative I global data sets: surface boundary conditions and atmospheric forcings for land-atmosphere studies. Bull Am Meteorol Soc 77: 1987–2003

Soriano A (1983) Deserts and semi-deserts of Patagonia. In: West NE (ed) Ecosystems of the world, vol 5. Temperate deserts and semi-deserts. Elsevier, Amsterdam, pp 423–460

Soriano A (1992) Rio De La Plata grasslands. In Coupland RT (ed) Ecosystems of the world, vol. 8A. Natural grasslands. Introduction and western hemisphere. Elsevier, Amsterdam, pp 367–407

Sukumar R, Ramesh R, Pant RK, Rajagopalan G (1993) A $\delta^{13}C$ record of late Quaternary climate change from tropical peats in southern India. Nature 364: 703–706

Syverson JP, Nickell GL, Spellenberg RW, Cunningham GL (1976) Carbon reduction pathways and standing crop in three Chihuahuan Desert plant communities. Southwest Nat 21: 311–320

Takeda T (1988) Studies on the ecology and geographical distribution of C_3 and C_4 grasses. IV. Geographical distribution of subfamily Bambusoideae in the world (in Japanese). Jpn J Crop Sci 57: 449–463

Takeda T, Tanikawa T, Agata W, Hakoyama S (1985a) Studies on the ecology and geographic distribution of C_3 and C_4 grasses (in Japanese) Jpn J Crop Sci 54: 54–64

Takeda T, Ueno O, Samejima M, Ohtani T (1985b) An investigation for the occurrence of C_4 photosynthesis in the Cyperaceae from Australia. Bot Mag Tokyo 98: 393–411

Teeri JA, Stowe LG (1976) Climatic patterns and the distribution of C_4 grasses in North America. Oecologia 23: 1–12

Tieszen LL, Senyimba MM, Imbamba SK, Troughton JH (1979) The distribution of C_3 and C_4 grasses and carbon isotope discrimination along an altitudinal and moisture gradient in Kenya. Oecologia 37: 337–350

Tieszen LL, Reed BC, Bliss N, Wylie BK, DeJong DD (1997) NDVI, C_3 and C_4 production, and distributions in the Great Plains grassland land cover classes. Ecol Appl 7: 59–78

Ting-Cheng Z (1993) Grasslands of China. In: Coupland RT (ed) Ecosystems of the world, vol. 8B. Natural grassland. eastern hemisphere and resume. Elsevier, Amsterdam, pp 61–82

Walter H, Box EO (1983) The deserts of central Asia. In: West NE (ed) Ecosystems of the World, vol 5. Temperate deserts and semi-deserts. Elsevier, Amsterdam, pp 193–236

Watson L, Dallwitz MJ (1992) The grass genera of the world. CAB International, Wallingford

Werger MJA (1986) The Karoo and southern Kalahari. In: Evenari M, Noy-Meir I, Goodall DW (eds) Ecosystems of the world, vol 12B. Hot deserts and arid shrublands. Elsevier, Amsterdam, pp 281–359

Wong SC, Cowan IR, Farquhar GD (1979) Stomatal conductance correlates with photosynthetic capacity. Nature 282: 424–426

Woodrow IE, Berry JA (1988) Enzymatic regulation of photosynthetic CO_2 fixation in C_3 plants. Annu Rev Plant Physiol 39: 533–594

Wyk JJP (1979) A general account of the grass cover of Africa. In: Numata M (ed) Ecology of grasslands and bamboolands in the world. Junk, The Hague, pp 124–132